Deformability of lap splices in RC structural walls

C. Kerby & S. Pujol
University of Canterbury, Christchurch

ABSTRACT

Severe structural damage associated with lap splices located near the foundation of reinforced concrete (RC) structural walls has been recorded in the field after recent major earthquakes in Chile, New Zealand, and Taiwan. Multiple laboratory investigations completed in the last two decades have corroborated the potential of lap splices to cause structural damage. Strain concentrations occurring near lap splice ends can cause decreases in RC wall deformability and, as a result, compromise building seismic resilience. Post-earthquake field observations and experimental studies of splice failure or damages in RC walls are summarized. There have been only 20 tests on the deformability of flexural RC walls with non-staggered lap splices, and no tests of walls with staggered lap splices. Two methods, the plastic-hinge analogy and a method by Pollalis (2021), are shown to be unreliable for estimating the drift capacity these walls. Further experimental and numerical work is required to understand the deformability of RC walls with lap splices near sections where reinforcement may yield. In the meantime, such lap splices should be avoided in new construction.

1 INTRODUCTION

The overlapping of steel reinforcement bars, called a lap splice, is the traditional force-transfer method where continuous steel reinforcement cannot be used. Lap splices in tension transfer forces between spliced bars via the surrounding concrete. Lap splices can be non-staggered or staggered, defined by the relative position of adjacent splice ends in a group of bars. Current design provisions encourage the staggering of lap splices.

Since the study of bond in concrete began in the early 20th century (Abrams, 1913), lap splices have been designed for sufficient strength to yield the lapped bars. Most 20th-century research on bond strength, and the factors affecting it, is summarized in ACI 408R-03. Factors affecting bond strength include lap splice length, concrete and steel material properties, clear cover, confining reinforcement, and bar diameter. Few experiments report displacements at splice failure, limiting the understanding of the deformability of lap splices. Deformability is critical in the design of lap splices, as splice failures are brittle, and can even be explosive (Hardisty et al., 2015).

Figure 2: The Alto Rio building after the 2010 Maule, Chile Earthquake (Song et al., 2012)

Figure 2: The collapsed Four Seasons Apartments after the 1964 Anchorage (USA) earthquake

In reinforced concrete (RC) walls, one convenient location for lap splices is also the most critical: just above the foundation where forces induced by seismic events are the largest. This discussion centres on lap splices of the main (vertical) reinforcement, which are most critical in in-plane "slender" RC walls. Slender RC walls can be defined by a height-to-length aspect ratio larger than 3.0. Slender RC walls deform primarily in flexure, inducing high forces in lap splices located near the wall extreme tension and compression fibres. The current NZ RC standard, NZS3101:2006-A3, allows staggered lap splices near earthquake-resistant wall foundations, while standards such as ACI318-19 in the USA and NCh430.Of2021 in Chile recently banned lap splices in boundary element reinforcement near wall foundations. It is important to discuss the deformability problems that lap splices create in RC walls to 1) improve displacement-driven design of new buildings in New Zealand and 2) to assess the seismic vulnerability of existing slender RC walls built over decades worldwide.

2 FIELD OBSERVATIONS

Table 1 provides a list of notable post-earthquake observations of damages to structures associated with lap splices. The most infamous of this list are the total collapses of the Alto Rio Building during the 2010 Maule earthquake (Figure 1) and the Four Seasons Apartments during the 1964 Anchorage earthquake (Figure 2). Lap splices were not always the exclusive reason for the listed failures but were major contributors in all cases. In structures that do not collapse, damages associated with lap splices can justify demolition.

During the 2010-2011 Canterbury Earthquakes, a RC wall failed at the top of a set of lap splices located at the foundation of a 13-story apartment building constructed in 1999 (Sritharan et al., 2014), suggesting problems caused by strain concentrations at lap splice ends. The transverse reinforcement confining the splices terminated in 90-degree hooks. The building did not collapse during either earthquake but was demolished soon after. Repeated field observations of severe damages associated with lap splices have been documented in reconnaissance reports for decades, especially since the 1990's. These observations have been corroborated by experimental studies in the last two decades.

3 EXPERIMENTAL WORK

There have been 10 experimental programmes of slender RC walls with lap splices to date (Aaleti et al., 2013; Almeida et al., 2017; Bimschas, 2010; Birely, 2012; Elnady, 2008; Hannewald et al., 2013; Layssi & Mitchell, 2012; Paterson & Mitchell, 2003; Pollalis, 2021; Villalobos Fernandez, 2014). All specimens had non-staggered lap splices at their base. Only 6 of 20 had height-to-length aspect ratios ≥ 3.0, and 17 of 20 had aspect ratios ≥ 2.0. 11 of 20 walls were tested as cantilevers loaded at a single point, while 9 tests were of shortened wall stubs with both moment and lateral load applied to create moment diagrams representative

Table 1: Notable post-earthquake observations of damages or collapses associated with lap splices

Earthquake	Year	Reference	Structure	Description of Damages
Anchorage, USA	1964	Kunze et al. (1965)	Cordova Building	Core wall damage concentrated at reinforcement splice above the first floor
			504th Air Force Hospital	Local spalling near elevator-core shear wall lap splices in a crowded reinforcement region
			Four Seasons Apartments	Total collapse due to failure of lap splices of main reinforcement
San Fernando, USA	1971	Almeida et al. (2017)	Indian Hills Medical Centre	Vertical splitting cracks along lap splice lengths
Northridge, USA	1994	Birely (2012)	Indian Hills Medical Centre	Increased spalling along splice lengths near RC wall bases
Marmara, Turkey	2003	Kilic and Sozen (2003)	115m Chimney	Failure of lap splices 30-35m above foundation leading to total collapse
Chuetsu, Japan	2007	Kim and Shiohara (2012)	58m Chimney	Fracture, without collapse, 17.5m above ground at the section where 1) exterior vertical bars were lap spliced, 2) interior vertical bars terminated, and 3) transverse reinforcement spacing doubled
Maule, Chile	2010	Song et al. (2012)	Alto Rio Building	Separation of building from foundation leading to total collapse. Both lap splice failures and bar fractures occurred
		NIST (2021)	Festival Building	Boundary element lap splice failure
			Emerald Building	Spalling of concrete along exterior wall lap splice length
Canterbury, NZ	2010 - 2011	Sritharan et al. (2014)	Terrace on the Park Apartments	Reinforcement buckling wall failure, concentrated about the first-floor splice region. Lap splices of horizontal reinforcement failed away from the wall base
Meinong, Taiwan	2016	NCREE and Purdue (2016)	泰慶天廈 / King's Town High-rise	Spalling of concrete along first-floor wall lap splices

of larger aspect ratios. The walls had drift capacities (the horizontal displacement at which a wall has lost 20% of its peak lateral-load capacity divided by the shear span) smaller than 2.0% in all but one test.

Lap splices can cause concentration of damage near splice ends, depending on the design of the splice and transverse reinforcement. When splices failed in bond, a combination of splice failures and bar fractures were more commonly observed than exclusively splice failure (Almeida et al., 2017). Lap splice failure in in-situ RC walls can lead to overturning, as seen in the Alto Rio building (Song et al., 2012). All experimental results supported the conclusion that the presence of non-staggered lap splices near sections where reinforcement yields adversely affects deformability.

No experimental program to date has quantified the deformability of staggered lap splices, representing a large and critical research gap. The staggering of lap splices in seismic-resistant RC walls is currently practiced in New Zealand, and has been practiced for decades worldwide, with little regard to how variables such as stagger distance or the percent of bars lapped at a section can alter wall deformability. An experimental program testing full-scale cantilever walls is underway at the University of Canterbury to study the deformability of staggered lap splices in RC walls.

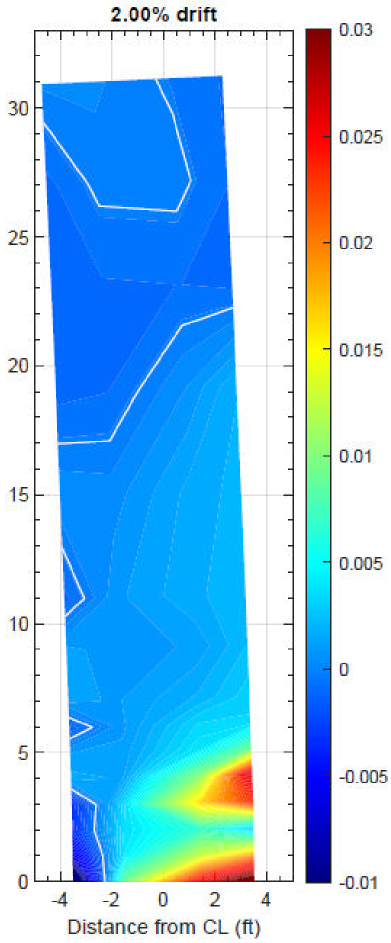

Figure 3: Surface strains of an RC wall with lap splices (Pollalis, 2021)

4 DEFORMATIONS OF SLENDER RC WALLS

4.1 The "Plastic-Hinge" and Lap Splices

The most popular approximation to estimate the drift capacity of RC walls is the "plastic-hinge" analogy for the wall curvature profile. The analogy concentrates inelastic curvatures in a region close to the section of maximum moment, most often the base of an RC wall (Blume et al., 1961). Despite its popularity in both research and industry, this approximation is crude even for structural walls without lap splices as it is based on the traditional definition of curvature at a section. This traditional definition of curvature does not consider observations showing that tensile surface strains in walls exhibiting inelastic response are distributed over a far greater length of the extreme fibres than compressive surface strains (Benavent Climent et al., 2012). No discernible correlation between measured drift capacity and drift capacity estimated using the plastic hinge analogy has been found, regardless of assumed plastic hinge length (Puranam et al., 2018). The plastic-hinge analogy can only consider a single failure mode, often concrete crushing. Transverse reinforcement and the presence of lap splices decrease the likelihood that concrete crushing will control failure over alternate failure modes such as reinforcement buckling or splice failure (Wang & Pujol, 2020).

The plastic-hinge analogy is even less applicable to slender RC walls with lap splices near the base. Figure 3 illustrates how inelastic strains can concentrate near the ends of lap splice in slender RC walls, rather than being distributed over a "plastic-hinge". Concentration of strains at lap splice ends was reported as early as 1945 (Kluge & Tuma). Wall drift capacities may be limited by the deformation capacity of the lap splices, not the crushing strain of the concrete as the plastic-hinge analogy suggests. Concentration of inelastic curvatures near lap splice ends renders the plastic-hinge analogy inapplicable to slender RC walls with lap splices near sections where reinforcement yields. The wall in Figure 3 had non-staggered boundary-element lap splices. There is no experimental data to confirm whether the strain concentration at splice ends in a wall with staggered lap splices would be of the same magnitude.

Buildings have been constructed worldwide with lap splices near the bases of RC walls for decades. It is quite possible that reconnaissance work after earthquakes has not accurately recorded damages associated with lap splices, instead attributing the damages to the development of a plastic-hinge region. In a collection of 183 photos of post-earthquake damages to slender RC walls from 1964 to 2010 by Birely (2012), 20% of images depicted damage at construction joints, the most convenient location for lap splices in RC walls. The experimental work summarized in Section 3 supports that lap splices often contribute to the failure of slender RC walls. New numerical models for RC walls are regularly published, but most have failed to account for the adverse effects of lap splices on deformability. Even existing models that consider the effects of lap splices only produce lower-bound estimates for drift capacity, as illustrated next.

4.2 Estimating Drift Capacity

Exsisting formulations do not produce consistent estimates of the drift capacity (DC) of RC walls with lap splices near their foundations. To illustrate this problem, two methods were used to estimate the drift capacity of 18 wall specimens from the experimental programs cited in Section 3. Properties of the selected walls are summarized in Table 2. All selected walls were rectangular in cross-section and symmetric in reinforcement. Both methods use the second moment-area theorem based on the assumed inelastic curvature profiles of Figure 4.

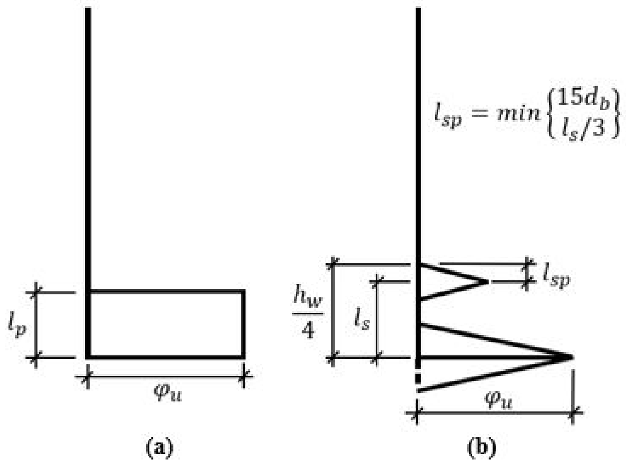

Figure 4: Assumed inelastic curvature distributions for (a) the plastic-hinge analogy and (b) the method by Pollalis (2021)

In the first method, the plastic-hinge analogy (Blume et al., 1961), inelastic curvatures are concentrated within a region of constant curvature above the base of the wall (Figure 4a). Elastic deformations were ignored. With this assumption, DC can be approximated as:

$$DC(\%) = \varphi_u l_p$$

where φ_u is the limiting curvature of the plastic hinge ($^{\varepsilon_{cu}}/_{c}$); l_p is the length of the plastic hinge, assumed to be half the length of the wall; c is the neutral axis depth from moment-curvature analysis; and ε_{cu} is the assumed limiting concrete compressive strain considering the effect of confinement (Puranam et al., 2018). Equation 1 produced unreliable, non-conservative estimates of DC for 13 of 18 wall tests (Figure 6a). Especially for wall specimens that failed in bond, Equation 1 grossly overestimated DC.

Pollalis (2021) developed an alternate method to estimate the deformability of RC walls according to the approximate curvature distribution of Figure 4b. For the sake of brevity, only portions of their multi-step method will be explained here. This approach implies that bond in non-staggered lap splices controls failure. An estimate of the expected peak bar stress (f_s) developed in non-staggered lap splices is calculated as:

$$f_s = 18\left(\frac{l_s}{d_b}\right)^{0.5} * f_{bc} * (k_{ts} + \frac{2}{3} - \frac{1}{k_{sf}}) \quad (2)$$

where l_s is the length of the splice; d_b is the diameter of longitudinal bars being developed; f_{bc} is the concrete contribution to bond strength; k_{ts} is a factor related to the magnitude of the peak bond stress expected along the splice (varying between $0.9 - 1.2$ for the walls of Table 2); and k_{sf} is a factor relating to the location of the peak bond stress (between $1.5 - 6.9$). Lower- and upper-bound limiting splice strains are estimated according to Figure 5 and the result for Equation 2. The average of the bounding strains obtained from Figure 5 was used to estimate φ_u and DC for the walls in Table 2. Alternatively, a different expression for f_s and stress-strain curves from tensile tests of reinforcement could be used to achieve a similar result. It is assumed in this discussion that the reinforcement properties of the walls in Table 2 are unknown. As presented here, Pollalis' method produced lower-bound estimates of drift capacity (Figure 6b).

Table 2: Properties of experimental slender RC walls with non-staggered lap splices selected for estimation of drift capacity

Test unit	Main references	Scale	f'_c	f_y	f_{ult}	l_s	d_{bl}	c_{min}	d_{bt}	s	h	L_w	DC Reported	ε_{cu}	DC Eq. 1	f_{bc}	f_s	ε_{ave}	DC Pollalis
-	-	-	MPa	MPa	MPa	d_{bl}	mm	mm	mm	mm	mm	mm	%	-	%	MPa	MPa	%	%
W1	Paterson and Mitchell (2003)	1:1	26	423	667	36	25	40	11	350	3250	1200	**0.8**	0.004	**2.4**	3.3	470	0.84	**0.3**
W2		1:1	33	423	667	36	25	40	11	350	3750	1200	**1.8**	0.017	**2.4**	3.6	500	1.80	**0.65**
CW2	Elnady (2008)	1:3	37	450	760	23	16	17	6	180	5000	1000	**0.2**	0.004	**1.4**	3.7	320	0.42	**0.25**
CW3		1:3	38	450	760	23	16	17	6	180	2250	1000	**0.3**	0.004	**1.4**	3.7	320	0.43	**0.15**
VK2	Bimschas (2010)	1:2	39	521	609	43	14	26	6	200	3300	1500	**0.9**	0.017	**1.3**	3.7	570	0.65	**0.2**
VK4	Hannewald et al. (2013)	1:2	39	521	609	43	14	26	6	200	3300	1500	**0.9**	0.017	**1.4**	3.7	570	0.65	**0.2**
VK5		1:2	35	521	609	43	14	26	6	200	4500	1500	**0.9**	0.017	**1.4**	3.6	560	0.63	**0.2**
W1*	Layssi and Mitchell (2012)	1:1	31	460	637	30	20	6	11	250	3250	1200	**0.4**	0.004	**3.2**	3.5	400	0.51	**0.15**
W2*		1:1	31	460	637	30	20	6	11	250	3250	1200	**0.4**	0.004	**2.3**	3.5	400	0.51	**0.15**
PW2	Birely (2012)	1:3	40	579	694	47	13	19	6	51	6710	3048	**1.1**	0.017	**1.2**	3.7	750	3.40	**1.0**
W-60-C	Villalobos Fernandez (2014)	1:1	31	461	655	61	25	19	6	64	3048	1520	**2.5**	0.016	**2.4**	3.5	610	3.60	**1.6**
W-40-C		1:1	31	461	655	41	25	19	6	64	3048	1520	**2.0**	0.016	**2.4**	3.5	610	3.60	**0.2**
W-60-N		1:1	34	461	655	61	25	19	10	127	3048	1520	**2.0**	0.017	**2.4**	3.6	630	4.40	**0.25**
W-60-N2		1:1	32	468	668	61	25	19	10	127	3048	1520	**1.5**	0.016	**2.4**	3.5	630	3.90	**0.25**
W60U	Pollalis (2021)	1:1	37	496	586	60	25.4	12.7	10	152	10058	2134	**1.9**	0.017	**1.9**	3.7	660	3.80	**1.45**
W80U		1:1	42	634	724	90	25.4	12.7	13	305	10058	2134	**2.0**	0.017	**1.5**	3.8	790	2.60	**0.65**
W60C		1:1	39	496	572	40	25.4	12.7	13	152	10058	2134	**2.0**	0.017	**1.9**	3.7	540	0.65	**0.35**
W80C		1:1	41	634	813	60	25.4	12.7	13	152	10058	2134	**2.5**	0.017	**1.5**	3.8	700	0.68	**0.25**

LEGEND:

f'_c = concrete cylinder strength in compression; f_y = reinforcement yield strength; f_{ult} = reinforcement ultimate strength; l_s = splice length; d_{bl} = longitudinal bar diameter; c_{min} = minimum cover to lapped bar surface; d_{bt} = transverse bar diameter; s = transverse reinforcement spacing; h = wall shear span; L_w = wall length; ε_{cu} = concrete limiting strain in compression; f_{bc} = concrete contribution to bond strength, per Pollalis (2021) Eq. 5.1; f_s = expected peak cross-sectional bar stress in a lap splice, per Eq. 2; ε_{ave} = limiting splice strain , per Figure 5 estimates of DC were conservative with 13 of 18 estimates being smaller than half the reported drift capacity. The method estimated lower bounds for DC, but the Figure 6b suggests it may be too conservative to be used in design.

Estimating the deformability of walls with lap splices remains a challenging problem. Neither the more common plastic-hinge analogy nor Pollalis' method produced estimates of DC consistent with measurements made in the 18 selected tests of slender RC walls with non-staggered lap splices of Table 2. The former method consistently overestimated DC while the latter underestimated it. Sources of uncertainty include material properties, cyclic stress-strain response of reinforcement, f_s at bond failure, and controlling failure mode. Lacking both experimental data and accurate numerical methods, more research is required on the deformability of slender RC walls with lap splices near their foundations.

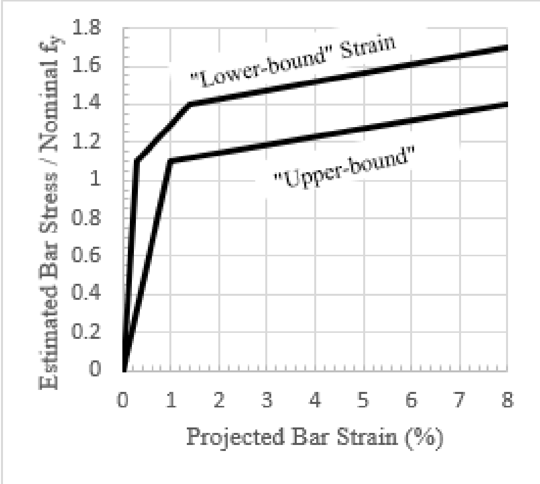

Figure 5: Ratio of estimated bar stress to nominal reinforcement yield stress (f_y) versus lower- and upper-bound lap spliced bar strains determined by Pollalis (2021)

5 CONCLUSIONS

Lap splices have been placed at the base of RC walls for decades. Repeated field observations and experimental tests have shown that lap splices near sections where reinforcement may yield can drastically reduce the deformability of slender RC walls. Concentrations of strains occur near the ends of yielded lap splices, preventing the distribution of inelastic deformations over large regions of the wall. Estimation of RC wall deformability is inconsistent with observation. More research is needed on the deformability of RC walls with staggered lap splices, including both additional experiments and work developing numerical methods accounting for the adverse effects of lap splices on wall deformability. Alternatively, lap splices

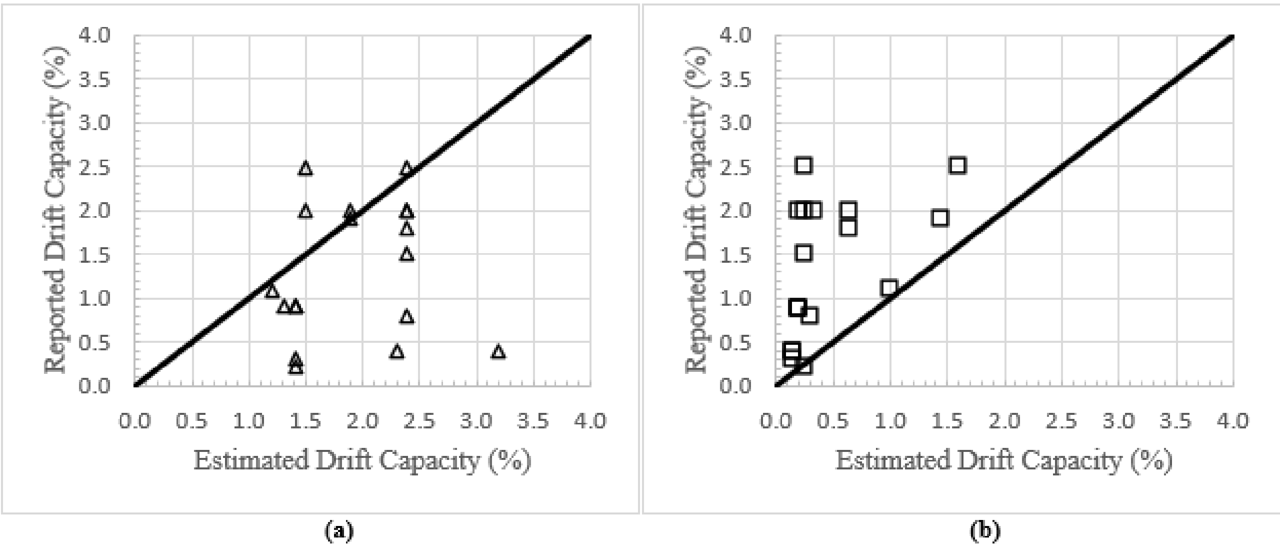

Figure 6: Reported drift capacity (%) from 18 tests of slender RC walls with non-staggered lap splices vs drift capacity (%) estimated using (a) Equation 1 and (b) Pollalis' method

should not be placed near sections where reinforcement is expected to yield.

REFERENCES

Aaleti, S., Brueggen, B. L., Johnson, B., French, C. E., & Sritharan, S. (2013). Cyclic response of reinforced concrete walls with different anchorage details: Experimental investigation. *Journal of Structural Engineering*, *139*(7), 1181-1191.

Abrams, D. (1913). *Test of bond between concrete and steel* (University of Illinois Bulletin: Engineering Experiment Station Issue 71).

Almeida, J. P., Prodan, O., Rosso, A., & Beyer, K. (2017). Influence of lap splices on the deformation capacity of rc walls. i: Database assembly, recent experimental data, and findings for model development. *ASCE J. Struct. Eng.*, *143*(12).

Benavent Climent, A., Escolano Margarit, D., Klenke, A., & Pujol, S. (2012). *Failure mechanism of reinforced concrete structural walls with and without confinement* 15 WCEEE, Lisoba.

Bimschas, M. (2010). *Displacement based seismic assessment of existing bridges in regions of moderate seismicity* ETH Zurich].

Birely, A. C. (2012). *Seismic performance of slender reinforced concrete structural walls* University of Washington].

Blume, J. A., Newmark, N. M., & Corning, L. H. (1961). *Design of multistory reinforced concrete buildings for earthquake motions* (Vol. 4). Portland Cement Association Chicago.

Elnady, E. M. M. (2008). *Seismic rehabilitation of RC structural walls* McMaster University].

Hannewald, P., Bimschas, M., & Dazio, A. (2013). Quasi-static cyclic tests on RC bridge piers with detailing deficiencies. *IBK Bericht*, *352*.

Hardisty, J. N., Villalobos, E., Richter, B. P., & Pujol, S. (2015). Lap splices in unconfined boundary elements. *Concr. Int*, *37*(1), 51-58.

Kilic, S. A., & Sozen, M. A. (2003). Evaluation of effect of August 17, 1999, Marmara earthquake on two tall reinforced concrete chimneys. *Structural Journal*, *100*(3), 357-364.

Kim, S., & Shiohara, H. (2012). Dynamic response analysis of a tall RC chimney damaged during 2007 Niigata-ken Chuetsu-Oki earthquake. 15th World Conf. on Earthquake Engineering,

Kluge, R. W., & Tuma, E. C. (1945). *Lapped bar splices in concrete beams*.

Kunze, W. E., Sbarounis, J. A., & Armhein, J. E. (1965). The March 27 Alaskan earthquake-effects on structures in Anchorage. ACI Journal Proceedings,

Layssi, H., & Mitchell, D. (2012). Experiments on seismic retrofit and repair of reinforced concrete shear walls. Proceedings of the 6th International Conference on FRP Composites in Civil Engineering (CICE),

NCREE, & Purdue. (2016). *2016 taiwan (meinong) earthquake*. https://datacenterhub.org/deedsdv/publications/view/534

NIST. (2021). *The 2010 chile earthquake: ground motion and building performance database*. https://disasterhub.nist.gov/resources/5

Paterson, J., & Mitchell, D. (2003). Seismic retrofit of shear walls with headed bars and carbon fiber wrap. *Journal of Structural Engineering*, *129*(5), 606-614.

Pollalis, W. G. (2021). *Drift Capacity of Reinforced Concrete Walls with Lap Splices* Purdue University Graduate School.

Puranam, A., Wang, Y., & Pujol, S. (2018). Estimating drift capacity of reinforced concrete structural walls. *ACI Structural Journal*, *115*, 1563-1574. https://doi.org/https://doi.org/10.14359/51702444

Song, C., Pujol, S., & Lepage, A. (2012). The collapse of the Alto Río building during the 27 February 2010 Maule, Chile, earthquake. *Earthquake Spectra*, *28*, S301-S334.

Sritharan, S., Beyer, K., Henry, R. S., Chai, Y. H., Kowalsky, M., & Bull, D. (2014). Understanding poor seismic performance of concrete walls and design implications. *Earthquake Spectra*, *30*, 307-334.

Villalobos Fernandez, E. J. (2014). *Seismic response of structural walls with geometric and reinforcement discontinuities* Purdue University].

Wang, Y., & Pujol, S. (2020). Effects of longitudinal reinforcement discontinuities on the seismic response of structural walls. *Bulletin of Earthquake Engineering*, *18*(15), 6735-6760. https://doi.org/10.1007/s10518-020-00963-4